Atmos. Meas. Tech. Discuss., 6, 8589–8602, 2013
www.atmos-meas-tech-discuss.net/6/8589/2013/
doi:10.5194/amtd-6-8589-2013

Atmospheric Measurement Techniques Discussions
Open Access

Effects of solar activity and geomagnetic field on noise in CALIOP profiles above the South Atlantic Anomaly

V. Noel[1], H. Chepfer[2], C. Hoareau[3], M. Reverdy[3], and G. Cesana[3]

[1]CNRS/Laboratoire de Météorologie Dynamique, UMR8539, CNRS, Institut Pierre-Simon Laplace, Ecole Polytechnique 91128 Palaiseau, France
[2]UPMC/Laboratoire de Météorologie Dynamique, Institut Pierre-Simon Laplace, Ecole Polytechnique 91128 Palaiseau, France
[3]Laboratoire de Météorologie Dynamique, Institut Pierre-Simon Laplace, Ecole Polytechnique 91128 Palaiseau, France

Received: 30 August 2013 – Accepted: 20 September 2013 – Published: 27 September 2013

Correspondence to: V. Noel (vincent.noel@lmd.polytechnique.fr)

Published by Copernicus Publications on behalf of the European Geosciences Union.

Abstract

By documenting noise levels in 6.5 yr of nighttime measurements by the spaceborne lidar CALIOP above the South Atlantic Anomaly (SAA), we show they contain information about the evolution of upwelling high-energy radiation levels in the area. We find the amount of noisy profiles is influenced by the 11 yr cycle of solar activity, fluctuates by ±5 % between 2006 and 2013, and is anticorrelated with solar activity with a 1 yr lag. The size of the SAA grows as solar activity decreases, and an overall westward shift of the SAA region is detectable. We predict SAA noise levels will increase anew after 2014, and will affect future spaceborne lidar missions most near 2020. In other areas, supposedly unaffected by incoming sunlight, nighttime noise levels are much weaker but follow the same 11 yr cycle, superimposed with a one-year cycle that affects both hemispheres similarly and could be attributed to geomagnetic activity.

1 Introduction

The South Atlantic Anomaly (SAA) refers to an irregular area, roughly centered on 30° W 30° S, extending over South America and the South Atlantic Ocean, where the Earth's geomagnetic field is weakest and the inner radiation belt comes closest to the surface. These conditions, due to the misalignment between the Earth's magnetic and rotational axes, lead to the trapping of ionized particles between 200 and 1600 km above the surface (Ginet et al., 2007) – mostly protons and electrons but also antiprotons created by the interaction with cosmic rays (Adriani et al., 2011). The energetic particles lead to an increase in outgoing radiation, affecting spaceborne electronics and detectors overflying the area.

The Cloud-Aerosol Lidar with Orthogonal Polarization (CALIOP, Winker et al., 2009) operates from within the A-Train constellation, which orbits the Earth at 705 km of altitude (Stephens et al., 2002). Its altitude and orbit make it travel through the SAA several times a day. It has been obvious since the early stages of CALIOP operation that

AMTD
6, 8589–8602, 2013

V. Noel et al.

the SAA strongly affected its nighttime observations of backscatter coefficients (Hunt et al., 2009, H09 hereafter), leading to increased levels of random fluctuations in the observed signal. Due to energetic radiations, dark noise levels in the 532 nm channel are 30 times larger in the SAA than elsewhere, leading to a decrease of the nighttime Signal-to-Noise ratio by a factor of 5 [H09].

The noise increase is especially noticeable in clear-sky areas at stratospheric altitudes, where backscatter returns are generally weak due to the absence of particles and low molecular densities compared to the troposphere. We performed a quick analysis of CALIOP data for 2008 and found that the standard deviation of stratospheric backscatter at 30–34 km is consistently 3.2 times larger over the SAA than over the rest of the globe. This has been proved particularly bothersome for the calibration of CALIOP signals based on stratospheric signals, which eventually had to ignore measurements over the area (Powell et al., 2009). Studies based on stratospheric CALIOP measurements require a careful attention to the area (e.g. Vernier et al., 2011; Lopes et al., 2013).

Here we document how changes in the intensity and spatial extent of the SAA across six and a half years (2006–2013) affect levels of dark noise in CALIOP observations at 532 nm. We show that within those noise levels are information about the evolution of the SAA with time.

2 Average extent of the SAA

H09 first described how telluric radiations in the SAA induce frequent current spikes and a significant amount of dark noise in CALIOP nighttime measurements. They mapped the profile-level dark noise at 532 nm during September and October 2006. They showed noise is also significant above the polar regions, approximately along the aurora ovals, where charged electrons precipitate from the magnetotail, flowing with the geomagnetic field. Finally, noise also increases at high latitudes, near the edges of nighttime orbits, as sunlight gets scattered above the horizon when the satellite

AMTD
6, 8589–8602, 2013

transitions from and to daytime. In those regions, noise levels are however much weaker than above the SAA.

Dark noise in CALIOP profiles can be tracked via the Parallel RMS Baseline at 532 nm variable, present in CALIOP Level 1 data files, which reports in digitizer counts the root mean square noise of 1000 15 m samples, calculated onboard from the 532 nm parallel channel in the 60.3–75.3 km altitude range (Hostetler et al., 2006). H09 showed digitizer counts generally stay below 100 in most areas, and reach their highest levels (> 2000) above the SAA. Figure 1 maps the percentage of individual CALIOP profiles at 333 m (from Level 1 data v.3.01) with dark noise digitizer counts above 200 in 2.5° × 2.5° grid boxes for 2007, the first available full-year of CALIOP data. Section 3 will describe how the SAA deviates from this baseline after 2007. The 200 threshold was selected after a sensitivity study showed that lower values still frequently appeared in random nighttime profiles. The patterns described by H09 are clear in Fig. 1. The fraction of profiles affected by strong noise is globally low, especially in the 40° S–40° N band. Only in the SAA are more than 30 % of profiles affected by such noise levels, and in its center all profiles are affected. Dark noise in the SAA reaches unique levels, often larger than 1000. The aurora ovals show up as wavy patterns at latitudes 50° and poleward, in which at most 25 % of profiles are affected by high noise levels. Increased noise due to sunlight scattering is faintly visible poleward of 35–40° in both hemispheres. The latitude bands affected by sunlight scattering follow a seasonal cycle, that in the Southern Hemisphere (SH) brings them near 40° S in January and down to 82° S in July. In the Northern Hemisphere (NH) the cycle is opposite. While this noise affected only two narrow latitude bands in the H09 monthly map, in Fig. 1 it is spread across a large latitude band (40°–82°) since the map covers an entire year. Boxes in Fig. 1 delimit regions that will be used in the next section: one strongly affected by the SAA (red), and three unaffected (green in the SH, orange in the NH, cyan around the equator). All these regions are supposedly too low in latitude to be directly affected by the sources of additional noise (sunlight scattering or polar noise) identified in H09 and described above.

In stark contrast to the clean geographical patterns of nighttime dark noise, we could not find meaning in the geographical distribution of daytime dark noise, which at first seem rather randomly distributed (not shown). This suggests that daytime dark noise levels are primarily affected by sunlight reflection on bright surface and low-level clouds, or reflection and scattering on ice crystals [H09]. In this configuration, increased daytime dark noise levels are triggered by favorable sun-cloud-detector geometries, which are quite random.

3 Evolution of the SAA

Figure 2 shows how the percentage of nighttime profiles affected by high noise levels (as defined in Sect. 2) deviate from the mean (57.5 %) across 15 days windows between June 2006 and December 2012 in the SAA region (red box in Fig. 1). CALIOP data come from Level 1 v.3.01 and 3.02 files, as available. The noisy fraction of profiles is minimum in 2006 (54 %), increases steadily to reach 60 % in 2010, then undergoes a rather abrupt drop in 2011 that brings it back to 2007 levels in early 2012 and onwards. Literature teaches us that the amount of radiation emitted from the SAA, which impacts the noise in CALIOP observations, is anticorrelated with the 11 yr cycle of solar activity (with 1 yr lag) (Furst et al., 2009). This anticorrelation is due to heating of the exo- and thermosphere during maximum solar activity, which leads to a higher neutral density in the altitudes below affected by the SAA (e.g. Qian et al., 2006). This increases the absorption and deflection of trapped particles, resulting in a lower particle flux compared to when the solar activity is minimum (Dachev et al., 1999). Thus the flux of energetic particles emitting radiations below CALIOP is smaller than during minimum solar activity. The 1 yr lag reflects the time needed for the atmosphere to react to incoming solar energy.

CALIOP began operating in 2006, during the downward section of solar cycle 23, when solar activity was already quite low compared to its 2000 maximum. It kept decreasing until 2009, while CALIOP noise levels over the SAA increased until 2010 due

AMTD
6, 8589–8602, 2013

to the 1 yr lag. Since then, solar cycle 24 has begun and solar activity has been increasing again, while noise in the SAA region decreased accordingly. The solar cycle is not symmetric: the increase in solar activity is faster (~ 3 yr) than the decrease, which shows as an opposite influence on noise levels (Fig. 2). We should thus expect the SAA noise to reach its minimum in the near future (probably in 2014), and resume a slow increase until the year following the next minimum of solar activity, in 2020. CALIOP will unfortunately be inoperative at this point, but it seems safe to assume that future spaceborne lidar missions will be similarly affected.

Since all profiles are noisy in the SAA center (Fig. 1) and the total number of noisy profiles in the SAA region changes with time (Fig. 2), the affected surface must change with time. Figure 3 shows the evolution with time of noisy profiles as a function of latitude (top) and longitude (bottom), in bands roughly centered on the SAA. The top figure shows that the SAA stayed roughly centered around 25° S, and more-or-less symmetrical except its north boundary shifted towards the Equator as the number of noisy profiles increased. The south boundary meanwhile appears constant, although it is weakly disturbed by the seasonal irruption (in December–January) of sunlight scatter. As a result, the SAA area zonally widened by roughly 2–3° after 2006 to reach a maximum extent in 2010. It quickly narrowed back to 2006 levels after 2011. The bottom figure shows that meridionally, the SAA region extended primarily westwards by roughly 5° until 2010, but narrowed primarily from the East after 2011. This translates to a slight westwards shift of the SAA between 2006 and 2013, which is consistent with predictions from the literature (e.g. Furst et al., 2009).

4 Noise levels in clear areas

In areas supposedly unaffected by sources of additional noise (non-SAA boxes in Fig. 1), the noisy fraction of profiles is extremely low on average (2 % ± 0.1 %) compared to inside the SAA. Even then, Fig. 4 (top) reveals the influence of the 11 yr solar cycle is quite noticeable in these regions, for the same reasons as over the SAA.

AMTD
6, 8589–8602, 2013

Intense solar activity warms up the high atmosphere, which leads to less charged particles overall and thus less noise, as in e.g. the relatively low-noise 2006–2008 period. Conversely, noise levels increase in periods of weak solar activity (2009–2010). Here, the increase is however extremely weak (less than a percent) compared to above the SAA. Figure 4 also reveals that noise levels in all three regions are affected by an underlying yearly cycle, which is minimum in July and maximum in January. Surprisingly, this cycle affects similarly both hemispheres with the season, and thus appears unrelated to the amount of incoming solar light reaching a particular hemisphere. This is contrary to our expectations for noise to be opposite in NH and SH (i.e. to follow the seasonal cycle of solar illumination). Peaks appear however more pronounced in the SH (green) and smoother in the NH (orange). In the latitude band where nighttime observations never directly experience solar illumination (30° S to 30° N), all longitudes outside of the SAA region show the same noise cycle. Noise levels in the SAA region are probably also affected, but the effect is too weak compared to the impact of the 11 yr solar cycle to register on Fig. 2.

A possible explanation for this cycle lies in the evolution of the geomagnetic field, which affects the amounts of charged particles that create background dark noise spikes in CALIOP data. The bottom pane of Fig. 4 shows the relative evolution of the deviation shown in the top pane (i.e. divided by the mean), detrended of solar cycle influence by subtracting the SAA equivalent (as in Fig. 2). Over-plotted in dark are relative deviations from the mean of the geomagnetic field intensity along the Earthward vector (He) measured by the magnetometers part of the Space Environment Monitor on the GOES-11 geostationary satellite (Singer et al., 1996). Note that their y-axis (right) is inverted to simplify visual comparison. CALIOP dark noise levels appear well anticorrelated with the geomagnetic field activity documented by GOES. Maximum anticorrelation (−0.67) is obtained when He measurements are delayed by 30 days. We have not identified the particular mechanism through which the geomagnetic field activity affects CALIOP noise levels.

AMTD
6, 8589–8602, 2013

5 Summary

By studying the evolution of noise in CALIOP nighttime profiles above the South Atlantic Anomaly region, we have found it influenced by the 11 yr cycle of solar activity. We documented how this area has been widening since 2006, shrunk since 2011 and overall shifted slightly to the West, in agreement with previous studies and predictions. Studies using CALIOP observations in the stratosphere and upper troposphere close to Central and South America should be mindful of the increased noise levels occurring in 2010–2011. We predict that SAA noise levels will soon start increasing again, and will affect future spaceborne lidar missions most near 2020. Moreover, we have shown that all CALIOP nighttime noise levels are influenced by the same 11 yr solar cycle, even in areas totally devoid of solar illumination. We have in addition identified an as-yet unexplained yearly noise cycle that appears unrelated to the seasonal change in solar illumination, but is anticorrelated with the geomagnetic field activity.

Acknowledgements. The authors wish to thank the NASA Langley CALIOP team for the CALIOP data, the ICARE data center for access to the data, and ClimServ for providing computing facilities. Data analysis was conducted using Python and Numpy (Oliphant, 2007). Figures were created using Matplotlib (Hunter, 2007).

The publication of this article is financed by CNRS-INSU.

AMTD

6, 8589–8602, 2013

Effects of solar activity and geomagnetic field

V. Noel et al.

References

Adriani, O., Barbarino, G. C., Bazilevskaya, G. A., Bellotti, R., Boezio, M., Bogomolov, E. A., Bongi, M., Bonvicini, V., Borisov, S., Bottai, S., Bruno, A., Cafagna, F., Campana, D., Carbone, R., Carlson, P., Casolino, M., Castellini, G., Consiglio, L., De Pascale, M. P., De Santis, C., De Simone, N., Di Felice, V., Galper, A. M., Gillard, W., Grishantseva, L., Jerse, G., Karelin, A. V., Kheymits, M. D., Koldashov, S. V., Krutkov, S. Y., Kvashnin, A. N., Leonov, A., Malakhov, V., Marcelli, L., Mayorov, A. G., Menn, W., Mikhailov, V. V., Mocchiutti, E., Monaco, A., Mori, N., Nikonov, N., Osteria, G., Palma, F., Papini, P., Pearce, M., Picozza, P., Pizzolotto, C., Ricci, M., Ricciarini, S. B., Rossetto, L., Sarkar, R., Simon, M., Sparvoli, R., Spillantini, P., Stozhkov, Y. I., Vacchi, A., Vannuccini, E., Vasilyev, G., Voronov, S. A., Yurkin, Y. T., Wu, J., Zampa, G., Zampa, N., and Zverev, V. G.: The discovery of geomagnetically trapped cosmic-ray antiprotons, Astrophys. J. Lett., 737, L29, doi:10.1088/2041-8205/737/2/L29, 2011.

Dachev, T. P., Tomov, B. T., Matviichuk, Y. N., Koleva, R. T., Semkova, J. V., Petrov, V. M., Benghin, V. V., Ivanov, Y. V., Semkova, J. V., Shurshakov, V. A., and Lemaire, J. F.: Solar cycle variations of MIR radiation environment as observed by the LIULIN dosimeter, Radiat. Meas., 30, 269–274, 1999.

Fürst, F., Wilms, J., Rothschild, R. E., Pottschmidt, K., Smith, D. M., and Lingenfelter, R.: Temporal variations of strength and location of the South Atlantic Anomaly as measured by RXTE, Earth Planet. Sc. Lett., 281, 125–133, doi:10.1016/j.epsl.2009.02.004, 2009.

Ginet, G. P., Madden, D., Dichter, B. K., and Brautigam, D. H.: Energetic proton maps for the South Atlantic Anomaly, in: Radiation Effects Data Workshop, IEEE, 1–8, doi:10.1109/REDW.2007.4342532, 2007.

Hostetler, C. A., Liu, Z., Reagan, J., Vaughan, M., Winker, D. M., Osborn, M., Hunt, W. H., Powell, K. A., and Trepte, C.: CALIOP algorithm theoretical basis document: calibration and level 1 data products, PC-SCI-201, available at: http://www-calipso.larc.nasa.gov/resources/project_documentation.php (last access: 27 September 2013), 2006.

Hunt, W. H., Winker, D., Vaughan, M. A., Powell, K. A., Lucker, P. L., and Weimer, C.: CALIPSO lidar description and performance assessment, J. Atmos. Ocean. Tech., 26, 1214–1228, 2009.

Hunter, J. D.: Matplotlib: a 2-D graphics environment, Comput. Sci. Eng., 9, 90–95, 2007.

AMTD
6, 8589–8602, 2013

Effects of solar activity and geomagnetic field

V. Noel et al.

Lopes, F. J. S., Landulfo, E., and Vaughan, M. A.: Assessment of the CALIPSO Lidar 532 nm version 3 lidar ratio models using a ground-based lidar and AERONET sun photometers in Brazil, Atmos. Meas. Tech. Discuss., 6, 1143–1199, doi:10.5194/amtd-6-1143-2013, 2013.

Oliphant, T. E.: Python for scientific computing, Comput. Sci. Eng., 9, 10–20, 2007.

Powell, K. A., Hostetler, C. A., Vaughan, M. A., Lee, K.-P., Trepte, C. R., Rogers, R. R., Winker, D. M., Liu, Z., Kuehn, R. E., Hunt, W. H., and Young, S. A.: CALIPSO lidar calibration algorithms. Part I: Nighttime 532 nm parallel channel and 532 nm perpendicular channel, J. Atmos. Ocean. Tech., 26, 2015–2033, doi:10.1175/2009JTECHA1242.1, 2009.

Qian, L., Roble, R. G., Solomon, S. C., and Kane, T. J.: Calculated and observed climate change in the thermosphere, and a predition for solar cycle 24, Geophys. Res. Lett., 33, L23705, doi:10.1029/2006GL027185, 2006.

Singer, H., Matheson, L., Grubb, R., Newman, A., and Bouwer, D.: Monitoring space weather with the GOES magnetometer, Proc. SPIE, 2812, 299–308, 1996.

Stephens, G. L., Vane, D. G., Boain, R. J., Mace, G. G., Sassen, K., Wang, Z., Illingworth, A. J., O'Connor, E. J., Rossow, W. B., Durden, S. L., Miller, S. D., Austin, R. T., Benedetti, A., Mitrescu, C., and Team, T. C. S.: The cloudsat mission and the a-train, B. Am. Meteorol. Soc., 83, 1771–1790, doi:10.1175/BAMS-83-12-1771, 2002.

Vernier, J.-P., Thomason, L. W., and Kar, J.: CALIPSO detection of an Asian tropopause aerosol layer, Geophys. Res. Lett., 38, L07804, doi:10.1029/2010GL046614, 2011.

Winker, D., Vaughan, M. A., Omar, A., Hu, Y., and Powell, K. A.: Overview of the CALIPSO mission and CALIOP data processing algorithms, J. Atmos. Ocean. Tech., 26, 2310–2323, 2009.

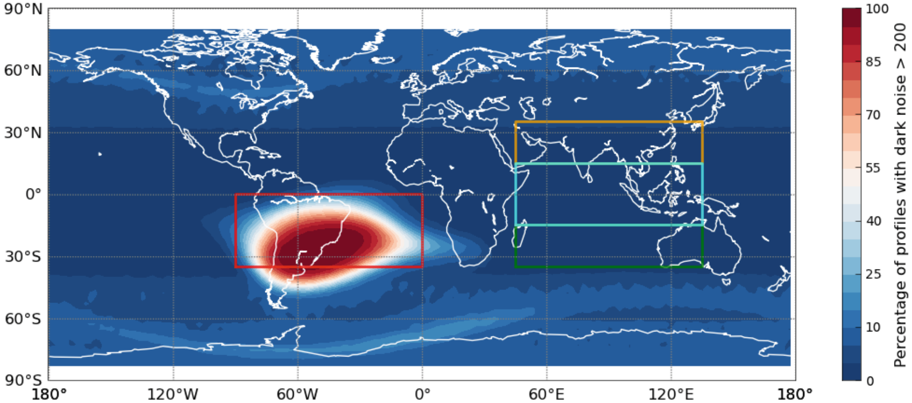

Fig. 1. Fraction (percents) of 333 m profiles with dark noise above 200 in 2.5° × 2.5° bins for all 2007 CALIOP nighttime observations. The red box delimits a region affected by the SAA but not directly affected by solar noise (top left: 90° W 0° S, bottom right: 0° W 35° S), The three boxes between 45° E and 135° E delimit regions unaffected by any recognized source of increased noise levels, in the South hemisphere (35° S to 15° S, green), the North hemisphere (15° N to 35° N, orange) and around the equator (15° S to 15° N, cyan).

Fig. 2. Deviation of the fraction of noisy 333 m profiles (dark noise above 200) from the mean over the entire period (57.5 %) in 15-days periods between 2006 and 2012 in the SAA region (red box in Fig. 1).

AMTD
6, 8589–8602, 2013

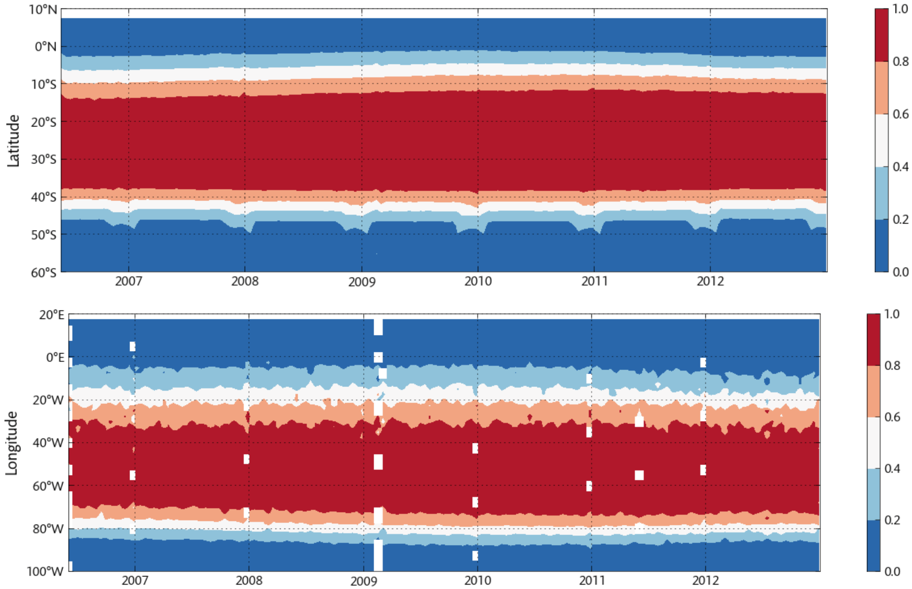

Fig. 3. Evolution with time of the fraction of noisy 333 m profiles as a function of latitude between 70° W and 30° W (top) and longitude between 40° S and 10° S (bottom). White boxes in the bottom figure are due to missing data.

AMTD
6, 8589–8602, 2013

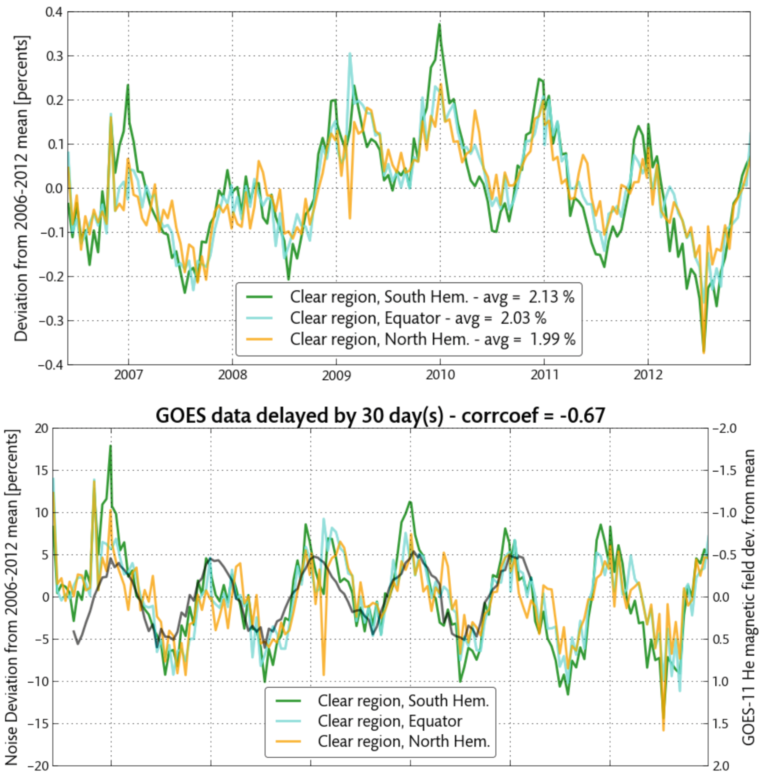

Fig. 4. (top) Same as Fig. 2, in areas supposedly unaffected by sources of additional noise (orange, green and cyan boxes in Fig. 1). (bottom) Same as top, but divided by the mean and detrended by subtracting the SAA relative deviation. The dark line shows the deviation of the geomagnetic field from the mean as documented by GOES (He field), delayed by 30 days. Note the y-axis (for GOES) is inverted.